Experimental Protocols for Studying Organic Non-Aqueous Redox Flow Batteries

Min Li, [†∥] *Susan A. Odom*[1]*,* [‡∥*] *Adam R. Pancoast,* [†∥] *Lily A. Robertson,* [§∥] *Thomas P. Vaid,* [#∥] *Garvit Agarwal,* [⊥∥] *Hieu A. Doan,* [⊥∥] *Yilin Wang,* [╫∥] *T. Malsha Suduwella,* [‡∥] *Sambasiva R. Bheemireddy,* [§∥] *Randy H. Ewoldt,* [╫∥] *Rajeev S. Assary,* [⊥∥] *Lu Zhang,* [§∥] *Matthew S. Sigman,* [†∥] *Shelley D. Minteer* [†∥*]

[†]Department of Chemistry, University of Utah, 315 South 1400 East, Salt Lake City, UT 84112, USA; [‡]Department of Chemistry, University of Kentucky, Lexington, Kentucky 40506, United States; [§]Joint Center for Energy Storage Research and Chemical Sciences and Engineering Division, Argonne National Laboratory, Lemont, Illinois 60439, United States; [#]Department of Chemistry, University of Michigan, Ann Arbor, Michigan 48109, United States; [╫] Department of Mechanical Science and Engineering, University of Illinois at Urbana-Champaign, Urbana, Illinois 61801, United States; [⊥]Joint Center for Energy Storage Research and Materials Science Division, Argonne National Laboratory, Lemont, Illinois 60439, United States; [∥]Joint Center for Energy Storage Research (JCESR), Lemont, Illinois 60439, United States;

AUTHOR INFORMATION

Corresponding Author

[1] Professor Dr. Susan Odom passed away unexpectedly on April 18, 2021.

Susan A. Odom, Email: susan.odom@uky.edu;

Shelley D. Minteer, Email: minteer@chem.utah.edu

Redox flow batteries (RFBs) are promising devices for grid-scale energy storage due to the decoupling of power and energy, which can be independently scaled by the electrode area and storage tank size, respectively (**Figure 1**).[1-3] To date, only aqueous RFBs, such as the vanadium RFB, have been implemented commercially. Nevertheless, the limited energy densities and high-cost materials may preclude their wider market penetration. Organic non-aqueous redox-flow batteries (O-NRFBs), which utilize redox-active organic molecules (ROMs)[4-6], have been offered as an attractive alternative. Many possible advantages include the use of earth-abundant elements (C, H, N, O, S, F), wherein the ROMs can be prepared from low-cost and sustainable materials.[7] Additionally, a large variety of electroactive moieties are accessible as building blocks, providing a synthetic platform to tune the properties of ROMs through rational design.[6] As a consequence, the development of novel ROMs has attracted researchers with diverse backgrounds prompting remarkable innovations in the past decade.[8-10] However, consistency in experimental protocols (e.g., electrochemical methods, cycling stability, experimental conditions) has not coincided with this uptick in research leading to sometimes ambiguous and incomparable results. This is further convoluted by the complexity innate to battery development, such as cell design, detection and characterization of reactions and active components. The O-NRFB application imposes stringent requirements on the physical or/and chemical processes involved in electrochemical cycling. Yet such considerations are often overlooked. Further, while quantum calculations provide a convenient tool for evaluating and selecting ROM candidates, this simulation is not always performed. Thus, in this ACS Viewpoint, we detail a means to standardize experimental protocols

for studies of O-NRFBs and suggest practices to facilitate fundamental understanding and development of ROMs.

1. Identification of Electroactive Molecule Candidates by Simulation and Computational Modeling

The past decade has seen tremendous progress in developing O-NRFBs.[2, 6, 11] Yet preparation of a ROM with long cycling lifetime is still challenging, as highlighted by a significant number of ROMs demonstrating >10% capacity decay within 100 cycles.[12-14] Further, there are complex tradeoffs in the optimization of electrochemical and physicochemical properties of ROMs.[14-16] Accordingly, developing experimental protocols for systematic investigation of ROM structure-property relationships is warranted and has been previously detailed.[3, 4, 11] Here, we do not seek to reiterate this discussion, but rather focus on experimental/computational procedures and how to apply these methods to produce accurate results to facilitate fundamental insights.

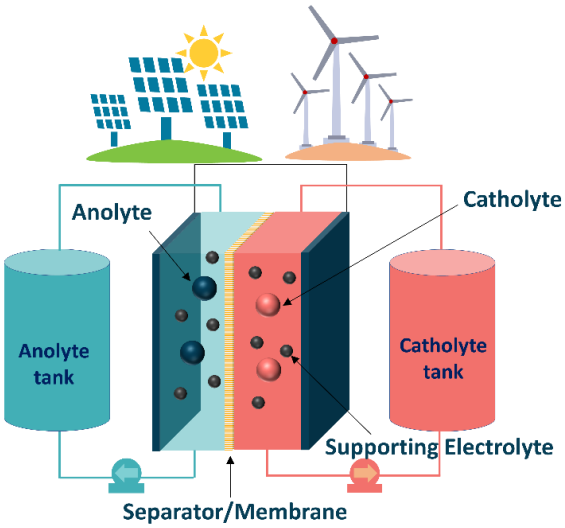

Figure 1. Schematic illustration of a redox flow battery. Anode and cathode materials are dissolved in solvents containing supporting electrolytes to form redox-active solutions called

anolyte and catholyte, respectively. A membrane is incorporated between the two half-cells to impede crossover of ROMs, while allowing transport of ions from supporting electrolytes to maintain charge balance. Pumps are used to flow the electroactive solutions between the electrochemical cells and the storage tanks.

Compared to the intuitional design, simulation and computational modeling provide an alternative, reliable, and economical approach to identifying ROM candidates for O-NRFBs prior to experiments.[14, 17, 18] Density Functional Theory (DFT) and Molecular Dynamics (MD) are often utilized to compute ROM properties; this is schematically shown in **Figure 2**.[8, 19, 20] Several commercial, scalable, and open-source codes for DFT (Gaussian 16, VASP, Quantum Espresso) and MD (LAMMPS, GROMACS) simulations are available. In many regards, redox potential is the first property of interest to be computed for ROMs for benchmarking the computational method. DFT has been shown to be robust for predicting the redox potentials of anolytes and catholytes, with mean absolute errors being about 0.10 V or less.[8, 21-24] In order to compute the redox potential of a molecule, the geometries of the neutral and reduced/oxidized states must be first optimized. Frequency calculations are subsequently carried out on those optimized geometries to obtain corresponding Gibbs free energies (G) at 298 K. The reduction (E_{red}) and oxidation (E_{ox}) potentials, in V with respect to the Normal Hydrogen Electrode (NHE), are then calculated as follows:

$$E_{red} = -\frac{G_{red} - G_{neu}}{nF} - NHE \qquad (1)$$

$$E_{ox} = \frac{G_{ox} - G_{neu}}{nF} - NHE \qquad (2)$$

where G_{red}, G_{ox}, and G_{neu} are the computed Gibbs free energies of the molecule in the reduced, oxidized, and neutral state of charge, respectively. F is the Faraday constant, n is the number of exchanged electrons, and NHE is the absolute potential of the normal hydrogen electrode.

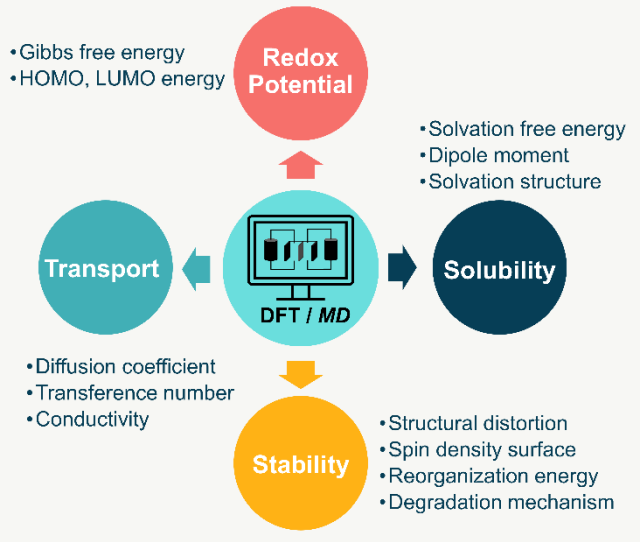

Figure 2. Predicted properties obtained by DFT and MD simulations.

As the concentration of ROMs is directly related to capacity and energy density, the ability to screen the solubility of neutral and charged ROM candidates is crucial. Solvation free energy allows for predicting solubility trends among a large number of derivatives from a molecule family.[25] Another approach to circumvent the complex theoretical evaluation of solubility, which requires the knowledge of accurate crystal structure and sublimation energy, is to use a regression model based on DFT-computed values with coefficients parametrized by experiments.[26] Often, MD is used to compute radial distribution functions and to simulate small-angle X-ray scattering (SAXS) spectra.[10, 19] These provide molecular-level insights into the bulk solvation structure of the solute, which can be used to understand solubility trends of different ROM species in non-aqueous solution.[10]

To include another critical design parameter – the stability of ROMs – several methods based on first principles calculations have been proposed.[17, 18] Perhaps the simplest approach is to investigate whether a molecule is susceptible to undesirable side reactions (e.g., ring-opening, de/re protonation, bond dissociation or formation) upon reduction/oxidation. The thermodynamics and kinetics of such decomposition reactions can be used for stability analysis. Alternatively, the spin density surface has been used as an indicator to evaluate the radical characters.[17, 18] The stability trend of ROMs can also be probed by the reorganization energy and root mean squared deviation (RMSD) between optimized coordinates of the neutral and oxidized/reduced states.[27] In general, redox-active species with lower reorganization energies can reach the charged states faster. Similarly, lower RMSD values indicate smaller structural distortion during electron transfer processes.[21]

To gain molecular level insights into the transport properties of ROMs in O-NRFBs, large scale classical MD simulations are routinely employed. Diffusivity, conductivity and transference number of different ROMs are often evaluated.[9, 28] The self-diffusion coefficients are computed using the Einstein relationship from the mean-squared displacement of the molecular species obtained from the MD trajectory. The computed diffusion coefficients at different temperatures can then be used to estimate the activation energy for diffusion using the Arrhenius relationship.[28] Additionally, the diffusion coefficients of the ionic species can be used to compute the transference number, which provides crucial insights into the relative contribution of the ionic species to the total conductivity of the solution.[9] Although MD simulations provide fundamental understanding of the effect of solvation structures on the properties of ROMs in O-NRFBs, their predictive capabilities are limited by the accuracy of the classical force-fields employed to model the complex interactions of various states of charge of the ROMs, the solvent and the supporting electrolyte

applied. Thus, rigorous experimental (or first principles-based) validation of MD simulations is often required, which makes it challenging to utilize these simulations for a wide range of electrolyte compositions and chemistries.

By utilizing the power of supercomputers, high-throughput DFT simulations have been carried out to accelerate ROM discovery for NRFBs.[8, 21, 25, 29] Typically, a molecular data set is first generated by incorporating various electron-donating groups (EDGs) and electron-withdrawing groups (EWGs) into a core structure at different substituted positions. Then, DFT is used to predict properties of interest. Promising candidates can then be suggested for experimental validation. Although performing high-throughput DFT calculations significantly speeds up the screening process compared to conducting experiments, the high computational cost and vast materials space often limit the size of a candidate pool to a few selected tens of thousands. To address this problem, Doan et al. combined high-throughput DFT simulations with active learning to efficiently explore a large molecular database for selecting redoxmer candidates.[8] Their active learning model based on Bayesian Optimization (BO) consists of two main components: a surrogate model and an acquisition function. Initially, the surrogate model takes a small set of known/DFT-computed data for training and then extrapolates on the remaining data set. The predicted values, together with their statistical uncertainties, are used by the acquisition function to rank the probability of improvement of any unknown candidate over the best current known one. Based on this ranking, new candidates can be selected for DFT evaluations and subsequently added to the existing training set. The surrogate model is trained again with the new set. The process repeats until meeting certain user-defined criteria (e.g., the optimal candidate is found). In their BO model, the authors successfully identified 42 homobenzylic ethers with the ideal redox

potentials out of a dataset of 112,000 molecules by performing DFT computations for a mere 100 molecules.[8]

Several limitations exist in DFT simulations for studying electrolytes in O-NRFBs. Dynamic interactions between solvent, supporting electrolyte, and ROMs at various concentrations play an important role in determining the properties of an electrolyte.[30] This is particularly important in modeling nonaqueous systems as these interactions tend to be complex due to the large and diverse chemical space of the organic components and their various possible combinations. In contrast, water as the only solvent can alleviate some of the difficulties of simulating the aqueous electrolyte environment. However, as the reduction and oxidation of the redox-active species in an aqueous electrolyte involves not only electrons but also protons, proper calibration of the computational model with various pH values is essential.[31] When many ROMs are investigated simultaneously, the redox potential calculations often neglect the presence of supporting electrolyte and treat the surrounding solvent molecules implicitly by invoking appropriate continuum models. Furthermore, the electrode/electrolyte interface is often unaccounted for when computing redox properties because of the many possible reactions among the electrolyte components at the electrode surface, wherein charge distribution and defects are important but challenging to model accurately. While these simplifications may only be valid for certain cases, e.g., low electrolyte concentration and reversible redox reactions, they are necessary for the compromise between speed and accuracy in high-throughput screenings.

2. Pre-Characterization of Synthesized ROMs

2.1. Solvents and Supporting Electrolytes – Drying and Purification

The lifetimes of organic charged intermediates are known to be detrimentally impacted by trace amounts of impurities, including oxygen, water or scavenging compounds.[32] By not proving the purity of new compounds and electrolyte reagents, reproducibility and published results are fallible. Tessensohn et al. performed a systematic study on commercially available nitrile solvents, drying procedures, and their effects on voltammetry experiments.[33] They found substantial impacts on ROM voltammetry dependent on suppliers and drying methods. Yet surprisingly, preparation of extra-dry or high-purity grade solvents and organic salts have not given adequate attention in O-NRFBs. To address the needs, we have summarized solvent and electrolyte purifying/drying procedures in the Supporting Information, and recommend researchers to perform similar in-house experiments to determine the best criterion for their needs.

To achieve credible battery results, we suggest fundamental characterization of ROMs guided by the "Compound Characterization Checklist" from the *Journal of Organic Chemistry*. While not every metric is needed for new ROMs, these analyses are: weight and percentage yield, physical state (including color), ^{1}H and ^{13}C NMR spectra, HRMS, elemental analysis, and copies of the NMR spectra. Optional but relevant characterization includes UV-vis in neutral or both states of charge, NMR spectra for any unique nuclei (e.g., ^{19}F), and X-ray characterization if suitable crystals form. Those preparing ionic ROMs should consider adding energy-dispersive X-ray (EDX) analysis to confirm ion metathesis.

2.2. Fundamental Electrochemical Studies of ROMs

2.2.1. Fundamental Redox Behavior by Cyclic Voltammetry

Cyclic voltammetry (CV) is a versatile tool for electrochemical characterization of ROMs. It should be noted that CV results are highly dependent on experimental conditions (e.g., scan

rate/direction, reference electrode, and the concentration of supporting electrolyte and ROMs).[34] Therefore, these conditions need to be explicitly stated and consistent throughout a data set to avoid any ambiguity. In particular, the potential of non-aqueous Ag^+/Ag reference depends upon variables such as the concentration of Ag^+, the identity of supporting electrolytes or solvents. Accordingly, it is advised that the Ag^+/Ag electrode is referenced against the ferrocene couple (vs. Fc^+/Fc) internally by adding a known concentration of Fc or externally by recording a CV of a solution with a known amount of Fc.

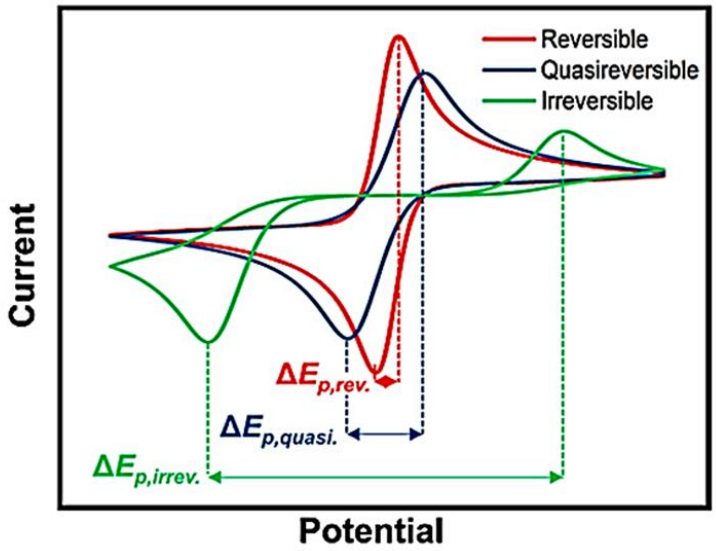

Figure 3. Schematic illustration of reversibility by CV. $\Delta E_{p,rev}$ = 59/n mV, $\Delta E_{p,rev} < \Delta E_{p,quasi} \leq 200/n\ mV$, $\Delta E_{p,irrev.} > 200/n$ mV, n is the number of electrons transferred in redox reaction. Reproduced from the ref. [35]. Copyright 2020 American Chemical Society.

Typically, CV is first applied to determine whether a particular ROM is suitable as a catholyte/anolyte based on the electrochemical and chemical reversibility (**Figure 3**). To establish the electrochemical reversibility of a redox process, the ratio of peak currents of the reduction and oxidation processes ($i_{p,a}$ and $i_{p,c}$, respectively) should be close to unity. Electrochemical

reversibility is indicated by the peak-to-peak separation (ΔEp); for a reversible electron transfer, this value should be close to 59 mV/n at 25 °C, where n is the number of electrons transferred.[36] It should be noted that overcompensating for IR losses can result in width < 59 mV.[36] In addition to the reversibility, repeatable CV scans (10 – 100 cycles) are encouraged to evaluate short-term stability of ROMs prior to cycling experiments.

Once good reversibility is obtained, redox potentials are subsequently calculated. Determination of the redox potential of a compound is typically done by reporting the average of the peak potentials ($E_{1/2}$). $E_{p/2}$, the half-peak potential – the potential at which the current is half the value of the peak current ($i_{p/2}$) – is sometimes used for irreversible electrochemical processes as an estimate of $E_{1/2}$. For further discussion on $E_{p/2}$ and $E_{1/2,}$ the reader is directed to the literature by Bard and Faulkner.[36]

Another important characteristic is the mass transport of ROMs (neutral and charged states) to and from the electrodes. A freely-diffusing compound should exhibit a linear correlation of $i_{p,a}$ and $i_{p,c}$ against the square root of the scan rate, as dictated by the Randles-Sevcik equation.[35] It is thus straightforward to determine the diffusion coefficient (D) by recording CV's at a range of different scan rates. For battery applications, a fast diffusional coefficient (>10^{-7} cm^2/s) is essential for battery operation.

Charge transfer at the electrode surface is another important electrochemical characteristic. The Nicholson method[37] and the Koutecký-Levich equation[38] are applied to evaluate the electron rate constant (k^o). For detailed theories and applications of these methods, the reader is directed to the reference.[35]

2.2.2. Self-Exchange Rates for Oligomers and Polymers

Oligomeric and polymeric ROMs have been developed to mitigate crossover when utilized in combination with size exclusion membranes (SEMs).[11] For this type of ROM, an important parameter is the self-exchange rate, which is a measure of how rapidly a molecule can redistribute charge among the uncharged portions of the oligomer/polymer.[39-41] Using a modified Randles-Sevcik equation (Eq.3, i_p = the peak current, n = number of electrons transferred, A = the area of the electrode, D_0 = the apparent diffusion coefficient, v = the scan rate, and $C_0\,\kappa$ = a constant that accounts for the exchange of cations into Nafion), it is possible to determine the apparent diffusion coefficient at different concentrations. A linear dependence upon concentration indicates considerable self-exchange is occurring. The Dahms-Ruff equations (Eq. 4 and 5) can then be used to determine the corresponding self-exchange rate.[39] In Eq. 4, D_{app} = the apparent diffusion coefficient, D_p = physical diffusion, and D_{et} = self-exchange diffusion. k_{ex} denotes the rate of self-exchange between ROM centers, δ = the distance between each redox active center in the ROM, and C_0^* the initial ROM concentration. High self-exchange rates can often compensate for sluggish diffusional profiles by yielding access to all the redox centers in the oligomer/polymer.

$$i_p = (2.69x10^5)n^{1.5}AD_0^{0.5}C_0^*v^{0.5}\kappa \qquad (3)$$

$$D_{app} = D_p + D_{et} \qquad (4)$$

$$D_{app} = D_{et} = \frac{k_{ex}\delta^2 C_0^*}{6} \qquad (5)$$

An example in this regard is the oligomerized cyclopropenium catholytes.[39] The rapid self-exchange rates (10^7-10^9 $M^{-1}s^{-1}$) enabled access to high states-of-charge (SOC) of 93-98% during cycling experiments. As such, although oligomers/polymers generally possess slower mass

transport relative to monomeric species, it is possible to access high SOCs by improving the self-exchange rates.

2.2.3. Permeability Analysis by CV

Crossover of active species is a major hurdle in O-NFRBs due to the non-ion selectivity of SEMs.[42] Quantifying crossover is thus an important metric that allows one to determine how permeable a particular membrane is with respect to a specific anolyte/catholyte.

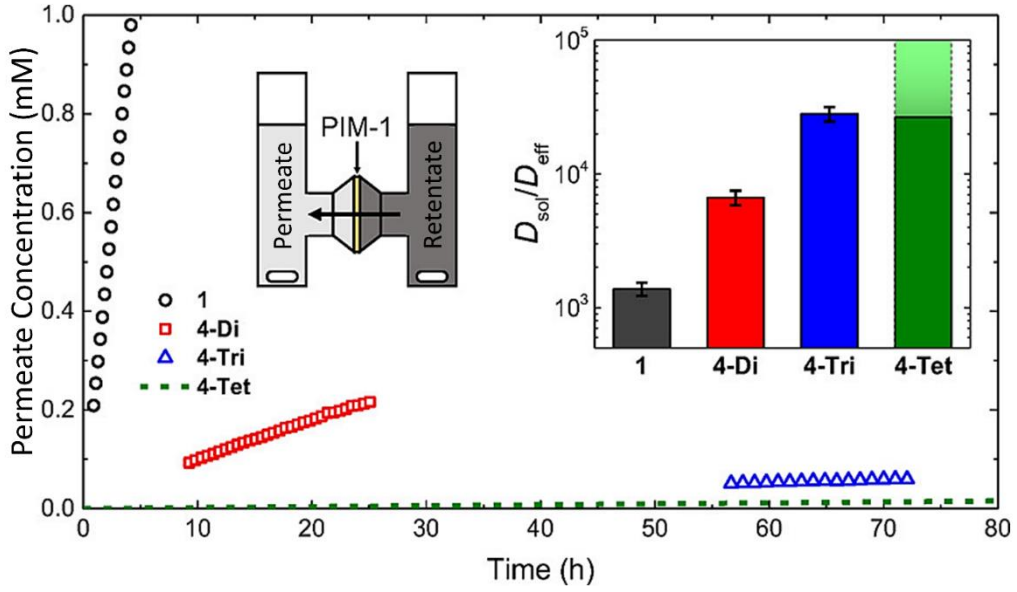

Figure 4. Illustration of using a H-cell for crossover. The inset shows the setup of the H-cell. Cyclopropenium (CP) oligomers (monomer **1**, dimer **4-Di**, trimer **4-Tri** and tetramer (**4-Tet**) were applied through a cross-linked polymer of intrinsic microporosity (PIM-1) membrane. the dashed line stands for the experimental detection limit; the graph inset indicates the calculated effective diffusion coefficients corrected for diffusion in solution. Adapted from the ref.[39]. Copyright 2018 American Chemical Society.

The permeability of a ROM through a membrane can be evaluated in an H-cell.[39, 43] As shown in **Figure 4**, the retentate side of an H-cell was loaded with electrolyte solution containing the compound of interest while the permeate solution was filled with an equal volume of solution containing only the supporting electrolyte. For an anolyte/catholyte with a counterion identical to those present in the supporting electrolyte, the amount of supporting electrolyte in the solutions should be adjusted to ensure osmotic balance. While stirring the solutions to ensure homogeneity, CVs were recorded at set time intervals and the peak current (i_p) was measured. The concentration of ROM that crossed over was determined from the calibration curve by taking advantage of the fact that i_p is directly correlated to ROM concentration as dictated by the Randles-Sevcik equation.[35] Permeability is then derived from the following equation:[44]

$$P = \frac{\ln\left(1 - \frac{2C_1}{C_2}\right)\left(-\frac{Vl}{2A}\right)}{t} \qquad (6)$$

where C_1 and C_2 are the ROM concentration in the retentate and permeate chambers, respectively ($\mathrm{mol/cm^3}$), V is the volume of solution ($\mathrm{cm^3}$), l is the thickness of the membrane (cm), A is the area of the membrane ($\mathrm{cm^2}$), and t is the time in seconds.

Researchers should note that while this permeability analysis via an H-cell is easy and informative, the concentration profile in an actual flow battery can vary more significantly over time. In addition, during the charge/discharge cycling, permeability driven by potential gradient can be non-trivial. Therefore, such analysis only provides preliminary results and additional measurements may be taken to validate the crossover in a flow cell setup.

In addition to CV to probe permeability,[39, 43] other alternative methods include UV-vis absorption spectroscopy,[45-47] and ^{1}H-NMR spectroscopy[48, 49] have been utilized to detect ROM

crossover in RFBs. Accordingly, researchers must choose the method best suited for their needs. Utilizing CV analysis to quantify the amount of crossover enables *in situ* analyses at mM concentrations of ROMs, making measurements of air-sensitive compounds facile provided the measurements are made under anaerobic conditions. However, for ROMs exhibiting low levels of crossover (≤ mM concentrations of ROMs), ^{1}H-NMR or UV-vis spectroscopy may be more suitable due to the higher sensitivity of these methods. Due to the typical *ex situ* nature of these methods, highly specialized experimental setups may be required for these systems when handling air-sensitive ROMs in order to maintain sample integrity. Additionally, samples containing open-shell species can be challenging to analyze via NMR spectroscopy due to their paramagnetic nature.

2.2.4. H-cell Cycling as a Stability Test of ROMs

To rapidly gauge the stability of ROMs, charge/discharge cycling experiments using 'H-cells' are often utilized prior to a flow cell experiment. These experiments can probe the stability of the catholyte or anolyte individually. The suggested protocols are included in the Section III of the Supporting Information.

Note that cell performance can be highly dependent on testing conditions and assessment methods.[11] It is important to include sufficient information about experimental methods and standardize data report to avoid biased conclusions. Brushett and Aziz have summarized recommended cycling methodology in the literature.[51, 52] Although these protocols center on aqueous systems, the principles are expected to be applicable to non-aqueous and other redox-active materials. Further, with suitable assessment approaches, one can peer into plausible decay mechanisms. Yao et al. discussed in detail about performance metrics and decay mechanisms of

all redox-active materials.[53] For example, time-denominated capacity decay indicates chemical decomposition, while cycle-denominated capacity decay may suggest electrochemical decomposition. When crossover becomes dominant, evaluation of both decay rates allows to evaluate whether the crossover results from one active species (oxidized or reduced) or both. Therefore, it is recommended to report time- and cycle- dependent capacity decays to assess ROM stability. Nevertheless, to fully understand degradation mechanisms, other analysis such as CVs and spectroscopic studies is often needed, which will be discussed in detail in Section 2.3.3 and Section 4.

Additionally, although H-cell cycling allows ROM stability to be evaluated in a short time period, the lack of flow force and the unique H-cell architecture might result in different performance profile in material utilization and crossover. Further, the variations between the membrane in an H-cell and a flow cell can also lead to different crossover results. Therefore, flow cell tests are suggested for further validation which will be discussed in the Section 3.

2.3. Investigation of Physicochemical Properties by Analytical Tools

2.3.1 Transport: Viscosity, Diffusivity, Conductivity

The working fluid in a flow battery must *flow*, therefore, viscosity, a measure of resistance to flow, is important to the performance of RFBs, *e.g.*, pumping pressure is directly related to the viscosity of the fluid. Viscosity is also the key transport property as viscous resistance fundamentally relates to diffusivity (*e.g.* the Stokes-Einstein equation), and together these relate to conductivity (*e.g.* the Nernst-Einstein equation). An ideal electrolyte in RFBs should have a sufficiently low viscosity (< 1,000 mPa),[54] high ionic diffusivity (1 x 10^{-7} to 3 x 10^{-5} cm^2/s),[55, 56]

and high conductivity (1 – 100 mS/cm)[56, 57] to decrease the operating costs and improve the working efficiency.

Dynamic viscosity, η, which is defined as the ratio of shear stress, τ, and shear rate, $\dot{\gamma}$, in a simple shear flow, is the most import property to measure. Typically, dynamic viscosity is directly measured with flow at known shear rate and stress conditions[58] using different flow geometrics, but it can also be determined by other means, *e.g.* inferred from diffusion measurements,[59] or from molecular simulations by looking at short time molecular relaxations.[60] Among the many flow geometries, we recommend closed-channel flow to avoid free surface effects such as evaporation, contamination, surface tension forces, and film formation at liquid-air interfaces.[61] A microfluidic viscometer m-VROC (RheoSense, Inc.) has been used to measure viscosity of ROM solutions, where the fluid is pushed by a syringe pump through a microfluidic slit. The working principle and analysis are detailed in Wang et al.[54]

2.3.2 Solubility

Flow battery capacity is directly proportional to the concentration of the active species, which is 1-1.5 M in vanadium RFBs. Unfortunately, a large number of ROMs developed exhibited solubility lower than 1 M. While some neutral ROMs have been reported to be miscible with organic electrolytes, their charged forms are usually less soluble.[62, 63] For example, the catholyte N-(2-(2-methoxyethoxy)ethyl)phenothiazine (MEEPT) is a liquid that is miscible with organic electrolytes, yet the solubility of the radical cation drops to 0.40 M for the BF_4^- salt.[63] Therefore, solubility in all SOCs needs to be considered. Approaches reported for determining the solubility of ROMs are described in detail in the Supporting Information.

Note that when analyzing the radical-ion materials, they must be quenched to transform the paramagnetic species into diamagnetic species so that the NMR spectrum does not have peak broadening. Sodium thiosulfate ($Na_2S_2O_3$) solid can be added in excess to reduce radical cations and other oxidized species, while I_2 will quench radical anions and other reduced species.

2.3.3 Stability

The stability of charged ROMs is usually the limiting factor in RFB performance. Both chemical and electrochemical stability are important. Electrochemical or cycling stability can be measured by H-cell or flow cell cycling. Chemical stability (also referred as 'calendar life') refers to the stability of the ROMs in their charged states irrespective of cycling behavior. Often, the two cannot be directly correlated.[64] Indeed, cycling stability of highly chemically stable ROMs may be limited by parasitic reactions caused by limitations in cell design[64] that could be improved by electrolyte/membrane choices.[65] Many analytical techniques can be used to probe the stability of charged states *ex situ*. *Ex situ* analysis can be performed for both cycling and calendar life studies, but this section will give an overview of these techniques in terms of chemical stability as that is most frequently studied.

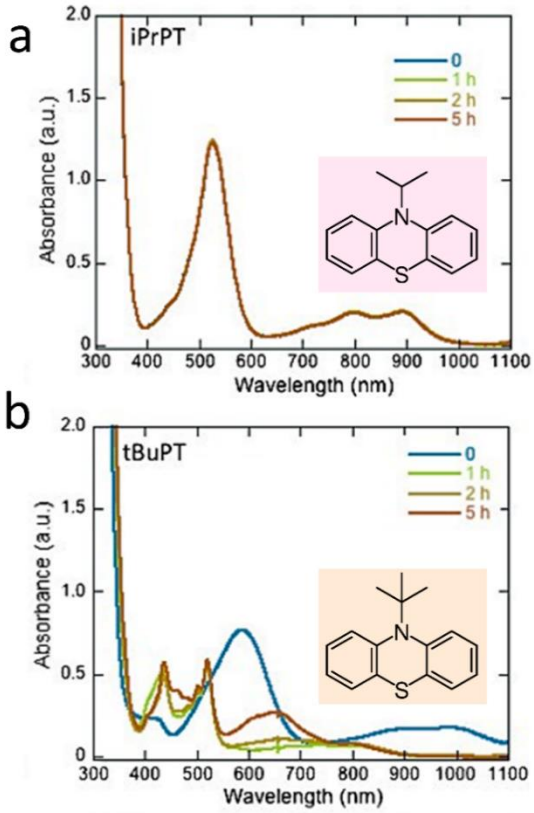

Figure 5. UV-vis spectra of the products of the reaction of the chemical oxidant magic blue with solutions of iPrPT (top) and tBuPT (bottom) at 0, 1, 2, and 5 h after generation in dichloromethane at 1.6 x 10^{-4} M. Reproduced from the ref.[66]. Copyright 2015 John Wiley & Sons, Inc.

UV-Vis Absorbance

ROMs used in O-NRFBs are mostly conjugated organic compounds that absorb light in the UV-vis region in both neutral and charged forms. When a charged state has features in the UV-vis that do not overlap with the neutral version, one may analyze stability by monitoring absorbance over time. Changes in the shape of the UV-vis spectrum are indicative of decomposition. One such example is the evaluation of the radical cation forms of a group of *N*-

substituted derivatives of phenothiazine.[66] In **Figure 5**, for the radical cation of *N-iso*-propylphenothiazine (iPrPT), generated by treatment with tris(4-parabromophenyl)aminium hexachloroantimonate (magic blue), the absorption spectrum remains largely unchanged over the 5 h. However, with *tert*-butylphenothiazine (tBuPT), the absorption spectrum changes with time, showing the formation of a new species, which, in this case, is the radical cation of unsubstituted phenothiazine.

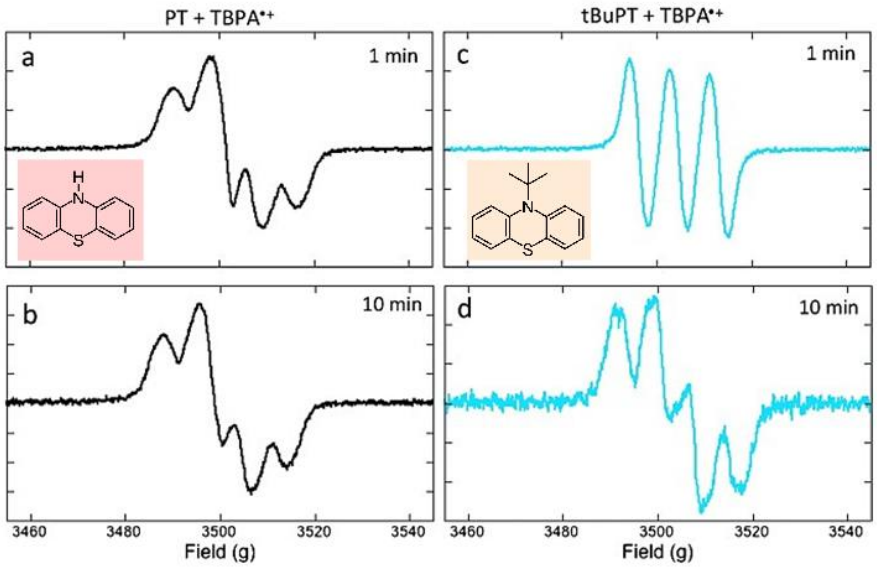

Figure 6. EPR spectra of dichloromethane solutions of tBuPT and PT generated at 1.6 x 10^{-4} M after treatment with the chemical oxidant magic blue at about 1 min after mixing (tBuPT,a; PT,c) and about 10 min after mixing (tBuPT, b; PT, d). Reproduced from the ref.[66]. Copyright 2015 John Wiley & Sons, Inc.

Electron Paramagnetic Resonance

Electron paramagnetic resonance (EPR) is used to identity charged states containing an unpaired electron and can be used to monitor species stability.[30, 57, 66] An example is shown in **Figure 6** wherein the radical cation of PT and of tBuPT were monitored over time.[66] Here, the shape of the PT radical cation remains largely unchanged over the 10 min between its generation and the acquisition of the second spectrum. However, the unstable radical cation of tBuPT decomposes, undergoing cleavage of the bond between the nitrogen atom and *tert*-butyl group to form the phenothiazine radical cation. In addition to comparing spectra at specific times, EPR can also be used to follow radical cation intensity over time, allowing half-lives to be extrapolated.[27, 30]

3. Evaluation of ROMs in RFBs

In RFBs, two reservoirs house the electrolytes, which are pumped through a charging station (**Figure S1**).[62] In the cell body, two casings house the flow fields, and gaskets and O-rings are used to prevent leakage between them and the carbon paper used for charging and the membranes or separators are placed in between the two electrolytes. In the case of membranes (e.g., Fumasep anion exchange membranes), crossover should be slow, while with porous separators (e.g., Celgard or Daramic), the electrolyte freely crosses over from one side of the cell to the other.

Flow cells for evaluation of ROMs can be symmetric or asymmetric. In an asymmetric cell, catholyte and anolyte are two distinct materials in their uncharged forms, which both become charged during cell cycling (**Figure 7a**). In contrast, symmetric cells contain the same materials in multiple SOCs (**Figure 7b**) or the same solution components in each half-cell (**Figure 7c-d**).

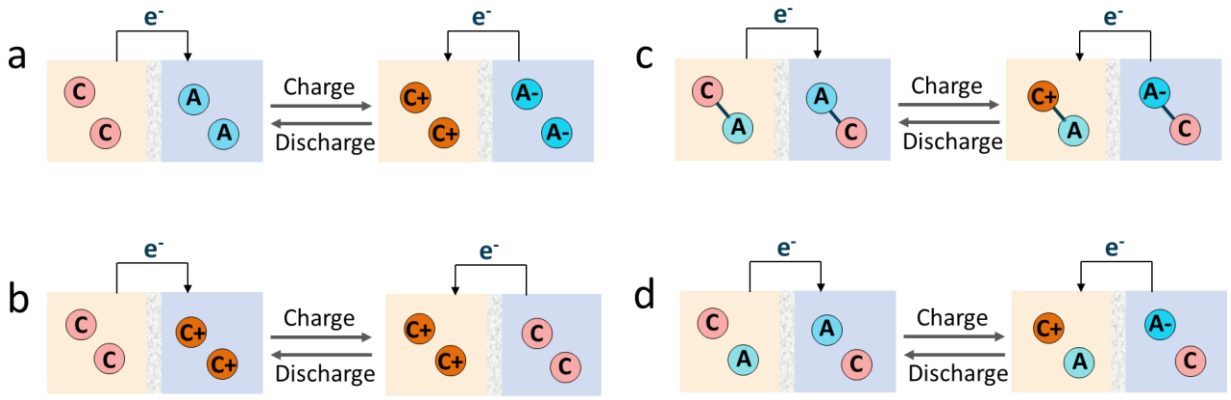

Figure 7. Representation of an asymmetric cell **(a)** and symmetric cells **(b-d)**. In the asymmetric cell, the charging process moves an electron from the catholyte to the anolyte. In the symmetric cell **b**, here shown for a catholyte (or anolyte) material, the charging process moves an electron from the neutral form to the cation. This cell stores no energy. In the symmetric cell **c**, the electroactive cores of catholyte and anolyte are covalently linked into one single structure, while in the symmetric cell **d**, a 1:1 molar ratio of catholyte and anolyte materials are physically mixed.

An asymmetric cell contains two distinct materials in two half-cells and is also called a full cell (**Figure 7a**). These cells represent the most realistic situation. However, they are subject to lifetime limitations of the less stable material. Compounds are subject to capacity fade as a result of ROM crossover, as well as efficiency losses when charged materials encounter each other and undergo self-discharge. As membranes that completely prevent ROMs from crossing over are not available yet, these losses are often observed in asymmetric cells. To improve, one can either operate with a non-selective separator with mixed catholyte/anolyte electrolytes to reduce the impact of species crossover, or alternatively use an ion-selective membrane. Oligomers with lower

crossover rates have been developed, and when paired with polymers of intrinsic microporosity (PIMs), crossover rates have been dramatically reduced.[39]

For a symmetric cell represented in **Figure 7b**, one side contains the pristine or neutral ROM, and the other side contains the charged form. During cell cycling, the uncharged state becomes charged, and the charged state is converted to its neutral state. An analogous arrangement can be made for a compound that is instead reduced.

The main advantage of evaluating ROMs in this symmetric cell is that only one material is evaluated.[67] This fact is beneficial in that the performance of a cell is not limited by the stability of the less stable species, the case in a full cell. A symmetric cell offers the greatest mimic of flow cell conditions in that all of the components of a flow cell – the electrodes, a separator or membrane, tubing and reservoirs – are all present. However, it should be noted that this cell design cannot store energy. Another configuration of this cell, useful for the evaluation of ROM stability, is the "unbalanced compositionally-symmetric flow cell" introduced by Aziz and coworkers.[68]

To mitigate ROM crossover while maintaining the capability of storing energy, symmetric cell designs indicated in **Figure 7c-d** have been developed.[12, 13, 69] In these cells, catholyte and anolyte are covalently linked into one single structure – bipolar redox-active molecules[5, 12, 69] (**Figure 7c**), or physically mixed in 1:1 molar ratio[13, 18, 70](**Figure 7d**). Consequently, ROM crossover driven by concentration gradient is significantly reduced. For more details, we have included case studies in applying symmetric and asymmetric flow cells in the Supporting Information. More recently solid electrolytes have been used as the membrane/separator in nonaqueous RFBs, and they present the great advantage that no crossover of ROMs is possible.[71, 72]

4. State-Of-Health Analysis and Interpretation of RFB Systems

4.1. Post Analysis of Plausible Decomposition Mechanisms

An O-NRFB will inevitably lose some amount of capacity during extended cycling. That capacity loss can occur through two major mechanisms: crossover of the ROMs through the membrane or separator (from the catholyte to the anolyte side or vice versa) or irreversible chemical decomposition of either one or both of the ROMs. In an asymmetric RFB, when either or both ROMs cross through the membrane to the other electrolyte solution, capacity is reduced as it is no longer available to be charged and discharged at the correct electrode. The remaining battery capacity will decrease and will be determined by the electrolyte solution containing the lesser amount of remaining ROM. In a symmetric RFB, crossover can still reduce battery capacity if the crossover is not symmetric and the amount of ROM on one side of the battery becomes limiting. The second major cause of capacity loss is decomposition, where a ROM is irreversibly converted to new chemical species. Because this reduces the amount of electroactive material available, it will also reduce capacity in both asymmetric and symmetric RFBs.

Post-run analysis of the electrolyte solutions by CV is a convenient method to monitor crossover and, in some cases, decomposition of the ROMs. To study such changes, CVs before cycling are taken to compare with post-run CVs. As CVs are mostly suitable for ROMs in the range of 1 to 10 mM, taking an aliquot of ROM solutions followed by a dilution is required for concentrated electrolyte solutions. If the pre- and post-run aliquots are diluted by the same factor and CVs are run under the same conditions, then information about relative concentration can be gained. An example is shown in **Figure 8**.[73] Both CVs are from the anolyte electrolyte solution of an asymmetric battery, with the dashed one taken before cycling and the solid one after cycling.

Before cycling, only the anolyte ROM was present in the CV, with two reversible reductions with $E_{1/2}$ of approximately -1.0 V and -1.6 V. After cycling, the CV showed that the concentration of the anolyte ROM was decreased. The decreased concentration of anolyte ROM can be either due to crossover to the catholyte electrolyte solution or decomposition. If the decomposed product is electroactive, it will be evident in the CV. For the present cell setup, both crossover and decomposition were evidenced in CVs – the presence of a small amount of a new species at about -0.75 V in the post-run CV indicated compound decomposition; and a new reversible wave at approximately +0.9 V indicated crossover of the positive ROM to the anolyte solution. Therefore, with pre- and post-cycling CVs of both the catholyte and anolyte electrolyte solutions, it is possible to get a full picture of crossover and decomposition that has occurred.

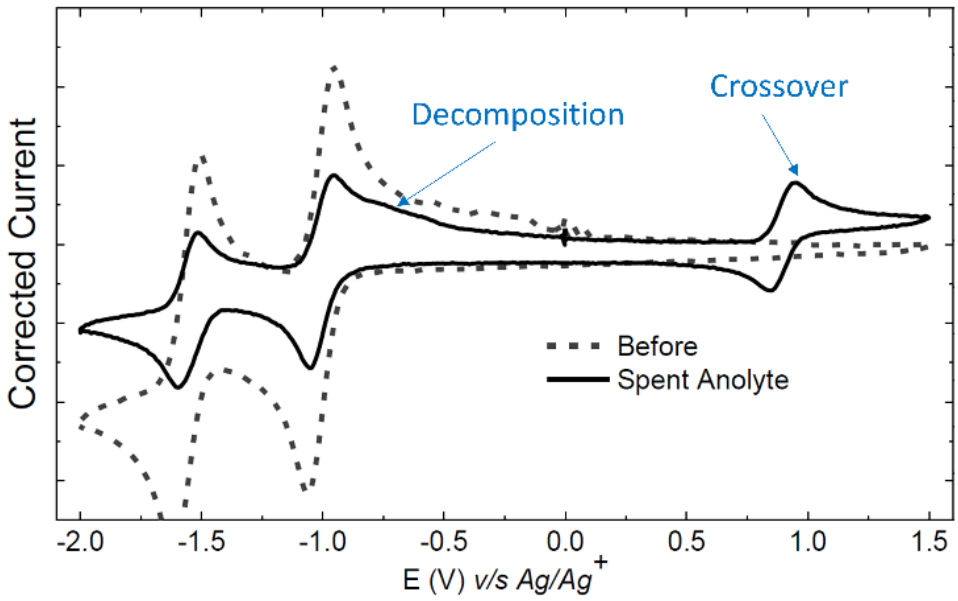

Figure 8. Cyclic voltammograms of the anolyte electrolyte solution before (dashed) and after (solid) cycling of a N-RFB, indicating a diminished concentration of anolyte ROM and crossover of the catholyte ROM during cycling. Adapted from the ref. [73]. Copyright 2020 John Wiley & Sons, Inc.

While CVs can probe information about crossover and decomposition of ROMs, they usually cannot yield information about the *identity* of decomposition products. Therefore, it is necessary to analyze the post-cycling electrolyte solution(s) by more informative techniques such as NMR spectroscopy and mass spectrometry (MS). Before this analysis, "quenching" of residue radicals to their most stable oxidation states is necessary. For example, if the negative ROM is a viologen, the viologen radical cation is likely to remain after cycling the electrolyte solution. The radical cation itself is paramagnetic and cannot be analyzed by NMR, but if it is oxidized to the dication by atmospheric oxygen in an uncontrolled manner, other products may arise that complicate analysis. Adding an oxidizing agent such as I_2 to the negative electrolyte solution will oxidize any viologen radicals present, along with related decomposition products, to the diamagnetic dication.[74]

In addition to radicals, another complication for decomposition analysis is the presence of a large amount of supporting electrolyte (often ≥ 0.5 M). When the supporting electrolyte includes organic cations as in tetrabutylammonium hexafluorophosphate (NBu_4PF_6), for example, analysis by ^{1}H and ^{13}C NMR is possible if the amount of ROM present is comparable to the concentration of the supporting electrolyte and the resonances of interest do not overlap with those of the NBu_4^+ (or other organic) cation. Otherwise, the spectra might be overwhelmed by the large signals from the NBu_4^+ cation. Suppression of the NBu_4^+ resonances in the NMR spectrum is possible, as is commonly done for non-deuterated solvents.[75] Alternatively, this issue often can be overcome when the ROM and the relevant decomposition products are neutrally charged organic molecules with moderate polarity. In such a case, the organic solvent is evaporated and the solid residue is extracted with diethyl ether, a solvent in which NBu_4PF_6 and similar supporting electrolytes have extremely low solubility. The extracted ROM and decomposition products can then be

concentrated and analyzed by NMR and MS. However, if the ROM (and its decomposition products) are ionic, separation from the supporting electrolyte can be difficult or even impossible. On the other hand, if the supporting electrolyte is completely inorganic (e.g., KPF_6), then interference with ^{1}H and ^{13}C NMR is not an issue and spectra can be obtained in a solvent such as d_6-DMSO with the supporting electrolyte present, though chemical shifts may be slightly different due to high salinity.

High-resolution mass spectrometry (HRMS) is very useful in identifying decomposition products of ROMs based on the molecular formula. Electrospray ionization (ESI) is the preferred method to transfer the analyte to the gas phase, as it usually leaves the molecules intact. If the ROM and decomposition products cannot be separated from the supporting electrolyte (organic or inorganic), this again presents an issue with interference in the analysis. However, we have found that at very high dilution, the ions of interest can be detected by ESI-HRMS, even in the presence of supporting electrolyte.[74]

4.2. In-situ Analysis by Spectro-Electrochemistry

While *ex-situ* detection is informative, it cannot provide a clear picture of the chemical evolution of various degradation components. Knowledge of this dynamic process may unravel the origins of the complex property metrics of ROMs, which in turn provides potential solutions to improve cell performance. This is especially true for intermediates, or short-lived species that may play a critical role in electrochemical cycling. The battery working conditions, however, makes *in situ* detection challenging, particularly for O-NRFBs. Efforts in online detection have been documented, including *in situ* detection of the SOC of ROMs by FTIR[12] and 'visualizing' crossover by fluorescent molecules,[76] but unfortunately, such devices remain to be developed.

Excitingly, *in situ* NMR devices have been recently reported and applied to the studies of two anthraquinone derivatives.[77] As aforementioned, NMR itself is a quantitative technique that allows for tracking the concentration and identity of chemical species at all phases. By sampling the species change over time, it is possible to learn how electrochemical reactions proceed at the atomic level. In the first attempt by Zhao et. al (indicated in **Figure 9a**), one cell compartment (either cathode or anode) is positioned next to the NMR magnet in such a way that the electrolyte solution flows through an NMR probe. This setup enables online monitoring of one specific ROM. The second attempt, as depicted in **Figure 9b**, uses a miniaturized flow cell placed inside of the NMR probe for simultaneous study of anolyte and catholyte. With these devices, Zhao and coworkers have successfully monitored battery self-discharge in real-time and revealed the process of electrolyte decomposition reactions. This example establishes the possibility of real-time monitoring of RFBs. Nevertheless, to be used in O-NRFBs, further modifications of these devices are required as charged ROMs can be highly oxygen- and moisture-sensitive. Additionally, considering that NMR cannot analyze paramagnetic species, development of in-situ EPR method can be advantageous for detection of free radicals generated in the electrochemical cycling. Recently, Zhao et al. coupled in-situ EPR and NMR to study redox flow batteries.[78] The coupled in-situ EPR enabled identifying of radical species and electron transfer rate between the singly and doubly reduced anthraquinone molecules, while the in-situ NMR revealed the decomposition reactions. Collectively, the degradation of ROM could be quantitatively corelated to the capacity fade observed in the flow cell.

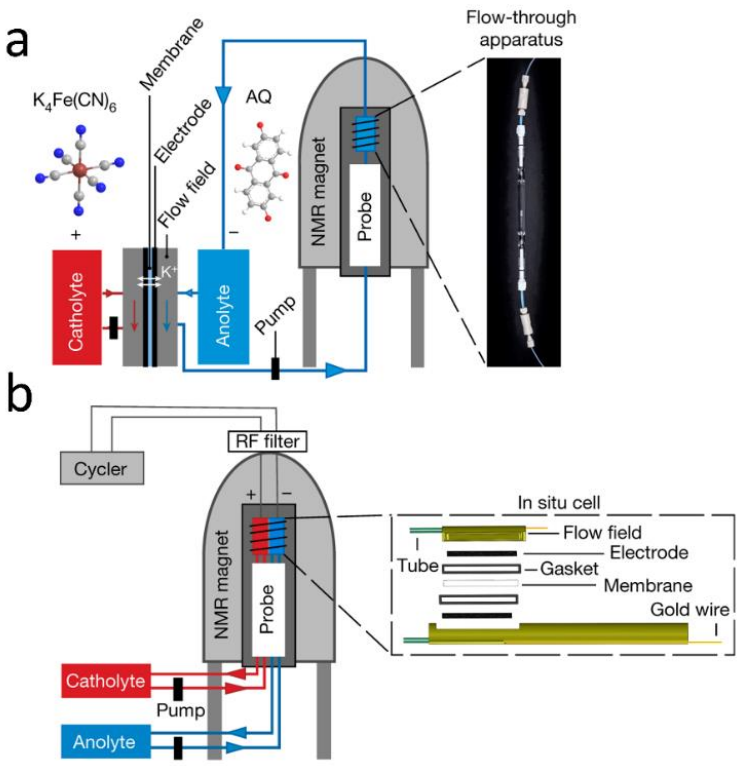

Figure 9. Schematic illustration of the *in-situ* NMR devices. **(a)** The in-situ NMR set up for monitoring one redox-active component. **(b)** Integration of flow cells with NMR probe for real-time analyzing battery charging/discharging process. Reproduced from the ref. [77]. Copyright 2020 Nature.

In summary, we have discussed and presented experimental protocols for studies of O-NRBFs. In recent years, the intersection of organic chemistry and battery science has led to exploration of a large variety of organic redox-active compounds. Although ROMs offer greater design flexibility and potentially more favorable properties in comparison to inorganic/vanadium species, the structure-property response of ROMs is complex and can be affected by various environmental parameters (e.g., impurities, electrochemical conditions). Yet, unfortunately, these experimental factors have not been giving adequate consideration. With the surge of interest in molecular screening of ROMs, it is imperative to establish rigorous experimental protocols and

standardize these procedures to obtain reliable battery results. Considering that synthesis and characterization are often time-consuming, we also suggest researchers integrate physical organic and computational chemistry for selecting ROM candidates. To further decrease the barrier of O-NRFBs for widespread implementation, the development of protocols for *in-situ* detection is still needed.

ASSOCIATED CONTENT

Supporting Information. Detailed methods for drying and purification of organic solvents and supporting electrolytes, solubility measurements and case studies for flow cell testing are included in the Supporting Information.

AUTHOR INFORMATION

Corresponding Authors

Susan A. Odom – Department of Chemistry, University of Kentucky, Lexington, Kentucky 40506, United States; Joint Center for Energy Storage Research, Lexington, Kentucky 40506, United States; orcid.org/0000-0001-6708-5852; Email: susan.odom@uky.edu

Shelley D. Minteer − Department of Chemistry, University of Utah, Salt Lake City, Utah 84112, United States; Joint Center for Energy Storage Research, Argonne, Illinois 60439, United States; orcid.org/ 0000-0002-5788-2249; Email: minteer@chem.utah.edu

Authors

Min Li – Department of Chemistry, University of Utah, 315 South 1400 East, Salt Lake City, UT 84112, USA; Joint Center for Energy Storage Research (JCESR), Argonne, Illinois 60439, United States; orcid.org/0000-0002-7791-6637;

Adam R. Pancoast − Department of Chemistry, University of Utah, Salt Lake City, Utah 84112, United States; Joint Center for Energy Storage Research, Argonne, Illinois 60439, United States.

Lily A. Robertson − Joint Center for Energy Storage Research and Chemical Sciences and Engineering Division, Argonne National Laboratory, Lemont, Illinois 60439, United States; orcid.org/0000-0002-8784-0568;

Thomas P. Vaid − Department of Chemistry, University of Michigan, Ann Arbor, Michigan 48109, United States; Joint Center for Energy Storage Research (JCESR), Argonne, Illinois 60439, United States; orcid.org/0000-0003-4597-0847;

Garvit Agarwal − Joint Center for Energy Storage Research and Materials Science Division, Argonne National Laboratory, Lemont, Illinois 60439, United States

Hieu A. Doan − Joint Center for Energy Storage Research and Materials Science Division, Argonne National Laboratory, Lemont, Illinois 60439, United States

Wang Yilin − Department of Mechanical Science and Engineering, University of Illinois at Urbana–Champaign, Urbana, Illinois 61801, United States; Joint Center for Energy Storage Research (JCESR), Argonne, Illinois 60439, United States

T. Malsha Suduwella − Department of Chemistry, University of Kentucky, Lexington, Kentucky 40506, United States; Joint Center for Energy Storage Research, Lexington, Kentucky 40506, United States; orcid.org/0000-0002-2349-7094;

Sambasiva R. Bheemireddy − Joint Center for Energy Storage Research and Chemical Sciences and Engineering Division, Argonne National Laboratory, Lemont, Illinois 60439, United States; orcid.org/0000-0003-1169-9649;

Randy H. Ewoldt − Department of Mechanical Science and Engineering, University of Illinois at Urbana–Champaign, Urbana, Illinois 61801, United States; Joint Center for Energy Storage Research (JCESR), Argonne, Illinois 60439, United States

Rajeev S. Assary − Joint Center for Energy Storage Research and Materials Science Division, Argonne National Laboratory, Lemont, Illinois 60439, United States; orcid.org/0000-0002-9571-3307;

Lu Zhang − Joint Center for Energy Storage Research and Chemical Sciences and Engineering Division, Argonne National Laboratory, Lemont, Illinois 60439, United States; orcid.org/0000-0003-0367-0862;

Matthew S. Sigman − Department of Chemistry, University of Utah, Salt Lake City, Utah 84112, United States; Joint Center for Energy Storage Research, Argonne, Illinois 60439, United States; orcid.org/0000-0002-5746-8830;

NOTES

The authors declare no competing financial interest.

ACKNOWLEDGMENT

The research was financially supported by the Joint Center for Energy Storage Research (JCESR), an Energy Innovation Hub funded by the U.S. Department of Energy, Office of Science, Basic Energy Sciences. The submitted manuscript has been created by UChicago Argonne, LLC, Operator of Argonne National Laboratory ("Argonne"). Argonne, a U.S. Department of Energy Office of Science laboratory, is operated under Contract No. DE-AC02-06CH11357. The U.S. Government retains for itself, and others acting on its behalf, a paid-up nonexclusive, irrevocable

worldwide license in said article to reproduce, prepare derivative works, distribute copies to the public, and perform publicly and display publicly, by or on behalf of the Government.

REFERENCES

1. Trahey, L.; Brushett, F. R.; Balsara, N. P.; Ceder, G.; Cheng, L.; Chiang, Y. M.; Hahn, N. T.; Ingram, B. J.; Minteer, S. D.; Moore, J. S.; Mueller, K. T.; Nazar, L. F.; Persson, K. A.; Siegel, D. J.; Xu, K.; Zavadil, K. R.; Srinivasan, V.; Crabtree, G. W., Energy storage emerging: A perspective from the Joint Center for Energy Storage Research. *Proc Natl Acad Sci U S A* **2020,** *117* (23), 12550-12557.

2. Ding, Y.; Zhang, C. K.; Zhang, L. Y.; Zhou, Y. G.; Yu, G. H., Pathways to Widespread Applications: Development of Redox Flow Batteries Based on New Chemistries. *Chem* **2019,** *5* (8), 1964-1987.

3. Luo, J. A.; Hu, B.; Hu, M. W.; Zhao, Y.; Liu, T. L., Status and Prospects of Organic Redox Flow Batteries toward Sustainable Energy Storage. *Acs Energy Lett* **2019,** *4* (9), 2220-2240.

4. Li, M.; Rhodes, Z.; Cabrera-Pardo, J. R.; Minteer, S. D., Recent advancements in rational design of non-aqueous organic redox flow batteries. *Sustain Energ Fuels* **2020,** *4* (9), 4370-4389.

5. Li, M.; Case, J.; Minteer, S. D., Bipolar Redox-Active Molecules in Non-Aqueous Organic Redox Flow Batteries: Status and Challenges. *Chemelectrochem* **2021,** *8*, 1-19.

6. Ding, Y.; Zhang, C.; Zhang, L.; Zhou, Y.; Yu, G., Molecular engineering of organic electroactive materials for redox flow batteries. *Chem Soc Rev* **2018,** *47* (1), 69-103.

7. Huskinson, B.; Marshak, M. P.; Suh, C.; Er, S.; Gerhardt, M. R.; Galvin, C. J.; Chen, X.; Aspuru-Guzik, A.; Gordon, R. G.; Aziz, M. J., A metal-free organic-inorganic aqueous flow battery. *Nature* **2014,** *505* (7482), 195-8.

8. Doan, H. A.; Agarwal, G.; Qian, H.; Counihan, M. J.; Rodríguez-López, J.; Moore, J. S.; Assary, R. S., Quantum Chemistry-Informed Active Learning to Accelerate the Design and Discovery of Sustainable Energy Storage Materials. *Chem Mater* **2020,** *32* (15), 6338-6346.

9. Li, Z. X.; Robertson, L. A.; Shkrob, I. A.; Smith, K. C.; Cheng, L.; Zhang, L.; Moore, J. S.; Z, Y., Realistic Ion Dynamics through Charge Renormalization in Nonaqueous Electrolytes. *J Phys Chem B* **2020,** *124* (15), 3214-3220.

10. Zhao, Y.; Sarnello, E. S.; Robertson, L. A.; Zhang, J.; Shi, Z.; Yu, Z.; Bheemireddy, S. R.; Z, Y.; Li, T.; Assary, R. S.; Cheng, L.; Zhang, Z.; Zhang, L.; Shkrob, I. A., Competitive Pi-Stacking and H-Bond Piling Increase Solubility of Heterocyclic Redoxmers. *J Phys Chem B* **2020,** *124* (46), 10409-10418.

11. Lai, Y. Y.; Li, X.; Zhu, Y., Polymeric Active Materials for Redox Flow Battery Application. *Acs Appl Polym Mater* **2020,** *2* (2), 113-128.

12. Duan, W. T.; Vemuri, R. S.; Milshtein, J. D.; Laramie, S.; Dmello, R. D.; Huang, J. H.; Zhang, L.; Hu, D. H.; Vijayakumar, M.; Wang, W.; Liu, J.; Darling, R. M.; Thompson, L.; Smith, K.; Moore, J. S.; Brushett, F. R.; Wei, X. L., A symmetric organic-based nonaqueous redox flow battery and its state of charge diagnostics by FTIR. *J Mater Chem A* **2016,** *4* (15), 5448-5456.

13. Wei, X. L.; Duan, W. T.; Huang, J. H.; Zhang, L.; Li, B.; Reed, D.; Xu, W.; Sprenkle, V.; Wang, W., A High-Current, Stable Nonaqueous Organic Redox Flow Battery. *Acs Energy Lett* **2016,** *1* (4), 705-711.

14. Yan, Y.; Robinson, S. G.; Sigman, M. S.; Sanford, M. S., Mechanism-Based Design of a High-Potential Catholyte Enables a 3.2 V All-Organic Nonaqueous Redox Flow Battery. *J Am Chem Soc* **2019,** *141* (38), 15301-15306.

15. Huang, J. H.; Duan, W. T.; Zhang, J. J.; Shkrob, I. A.; Assary, R. S.; Pan, B. F.; Liao, C.; Zhang, Z. C.; Wei, X. L.; Zhang, L., Substituted thiadiazoles as energy-rich anolytes for nonaqueous redox flow cells. *J Mater Chem A* **2018,** *6* (15), 6251-6254.

16. Milton, M.; Cheng, Q.; Yang, Y.; Nuckolls, C.; Hernandez Sanchez, R.; Sisto, T. J., Molecular Materials for Nonaqueous Flow Batteries with a High Coulombic Efficiency and Stable Cycling. *Nano Lett* **2017,** *17* (12), 7859-7863.

17. Montoto, E. C.; Cao, Y.; Hernandez-Burgos, K.; Sevov, C. S.; Braten, M. N.; Helms, B. A.; Moore, J. S.; Rodriguez-Lopez, J., Effect of the Backbone Tether on the Electrochemical Properties of Soluble Cyclopropenium Redox-Active Polymers. *Macromolecules* **2018,** *51* (10), 3539-3546.

18. Yan, Y.; Vaid, T. P.; Sanford, M. S., Bis(diisopropylamino)cyclopropenium-arene Cations as High Oxidation Potential and High Stability Catholytes for Non-aqueous Redox Flow Batteries. *J Am Chem Soc* **2020,** *142* (41), 17564-17571.

19. Shkrob, I. A.; Li, T.; Sarnello, E.; Robertson, L. A.; Zhao, Y.; Farag, H.; Yu, Z.; Zhang, J.; Bheemireddy, S. R.; Z, Y.; Assary, R. S.; Ewoldt, R. H.; Cheng, L.; Zhang, L., Self-Assembled Solute Networks in Crowded Electrolyte Solutions and Nanoconfinement of Charged Redoxmer Molecules. *J Phys Chem B* **2020,** *124* (45), 10226-10236.

20. Zhang, L.; Qian, Y.; Feng, R.; Ding, Y.; Zu, X.; Zhang, C.; Guo, X.; Wang, W.; Yu, G., Reversible redox chemistry in azobenzene-based organic molecules for high-capacity and long-life nonaqueous redox flow batteries. *Nat Commun* **2020,** *11* (1), 3843.

21. de la Cruz, C.; Molina, A.; Patil, N.; Ventosa, E.; Marcilla, R.; Mavrandonakis, A., New insights into phenazine-based organic redox flow batteries by using high-throughput DFT modelling. *Sustain Energ Fuels* **2020,** *4* (11), 5513-5521.

22. Marenich, A. V.; Ho, J.; Coote, M. L.; Cramer, C. J.; Truhlar, D. G., Computational electrochemistry: prediction of liquid-phase reduction potentials. *Phys Chem Chem Phys* **2014,** *16* (29), 15068-106.

23. McNeill, A. R.; Bodman, S. E.; Burney, A. M.; Hughes, C. D.; Crittenden, D. L., Experimental Validation of a Computational Screening Approach to Predict Redox Potentials for a Diverse Variety of Redox-Active Organic Molecules. *J Phys Chem C* **2020,** *124* (44), 24105-24114.

24. Lynch, E. J.; Speelman, A. L.; Curry, B. A.; Murillo, C. S.; Gillmore, J. G., Expanding and testing a computational method for predicting the ground state reduction potentials of organic molecules on the basis of empirical correlation to experiment. *J Org Chem* **2012,** *77* (15), 6423-30.

25. Cheng, L.; Assary, R. S.; Qu, X.; Jain, A.; Ong, S. P.; Rajput, N. N.; Persson, K.; Curtiss, L. A., Accelerating Electrolyte Discovery for Energy Storage with High-Throughput Screening. *J Phys Chem Lett* **2015,** *6* (2), 283-91.

26. Kucharyson, J. F.; Cheng, L.; Tung, S. O.; Curtiss, L. A.; Thompson, L. T., Predicting the potentials, solubilities and stabilities of metal-acetylacetonates for non-aqueous redox flow batteries using density functional theory calculations. *J Mater Chem A* **2017,** *5* (26), 13700-13709.

27. Zhang, J.; Shkrob, I. A.; Assary, R. S.; Tung, S. o.; Silcox, B.; Curtiss, L. A.; Thompson, L.; Zhang, L., Toward Improved Catholyte Materials for Redox Flow Batteries: What Controls Chemical Stability of Persistent Radical Cations? *J Phys Chem C* **2017,** *121* (42), 23347-23358.

28. Han, K. S.; Rajput, N. N.; Wei, X.; Wang, W.; Hu, J. Z.; Persson, K. A.; Mueller, K. T., Diffusional motion of redox centers in carbonate electrolytes. *J Chem Phys* **2014,** *141* (10), 104509.

29. Pelzer, K. M.; Cheng, L.; Curtiss, L. A., Effects of Functional Groups in Redox-Active Organic Molecules: A High-Throughput Screening Approach. *J Phys Chem C* **2017,** *121* (1), 237-245.

30. Zhao, Y. Y.; Yu, Z.; Robertson, L. A.; Zhang, J. J.; Shi, Z. X.; Bheemireddy, S. R.; Shkrob, I.; Li, T.; Zhang, Z. C.; Cheng, L.; Zhang, L., Unexpected electrochemical behavior of an anolyte redoxmer in flow battery electrolytes: solvating cations help to fight against the thermodynamic-kinetic dilemma. *J Mater Chem A* **2020,** *8* (27), 13470-13479.

31. Lin, K. X.; Gomez-Bombarelli, R.; Beh, E. S.; Tong, L. C.; Chen, Q.; Valle, A.; Aspuru-Guzik, A.; Aziz, M. J.; Gordon, R. G., A redox-flow battery with an alloxazine-based organic electrolyte. *Nat Energy* **2016,** *1* (9), 1-8.

32. Griller, D.; Ingold, K. U., Persistent Carbon-Centered Radicals. *Accounts Chem Res* **1976,** *9* (1), 13-19.

33. Tessensohn, M. E.; Ng, S. J.; Chan, K. K.; Gan, S. L.; Sims, N. F.; Koh, Y. R.; Webster, R. D., Impurities in Nitrile Solvents Commonly Used for Electrochemistry, and their Effects on Voltammetric Data. *Chemelectrochem* **2016,** *3* (11), 1753-1759.

34. Elgrishi, N.; Rountree, K. J.; McCarthy, B. D.; Rountree, E. S.; Eisenhart, T. T.; Dempsey, J. L., A Practical Beginner's Guide to Cyclic Voltammetry. *J Chem Educ* **2018,** *95* (2), 197-206.

35. Wang, H.; Sayed, S. Y.; Luber, E. J.; Olsen, B. C.; Shirurkar, S. M.; Venkatakrishnan, S.; Tefashe, U. M.; Farquhar, A. K.; Smotkin, E. S.; McCreery, R. L.; Buriak, J. M., Redox Flow Batteries: How to Determine Electrochemical Kinetic Parameters. *Acs Nano* **2020,** *14* (3), 2575-2584.

36. Bard, A. J.; Faulkner, L. R., Fundamentals and applications. *Electrochem Methods* **2001,** *2* (482), 580-632.

37. Nicholson, R. S., Theory and Application of Cyclic Voltammetry for Measurement of Electrode Reaction Kinetics. *Anal Chem* **1965,** *37* (11), 1351-+.

38. Treimer, S.; Tang, A.; Johnson, D. C., A consideration of the application of Koutecky-Levich plots in the diagnoses of charge-transfer mechanisms at rotated disk electrodes. *Electroanalysis* **2002,** *14* (3), 165-171.

39. Hendriks, K. H.; Robinson, S. G.; Braten, M. N.; Sevov, C. S.; Helms, B. A.; Sigman, M. S.; Minteer, S. D.; Sanford, M. S., High-Performance Oligomeric Catholytes for Effective Macromolecular Separation in Nonaqueous Redox Flow Batteries. *ACS Cent Sci* **2018,** *4* (2), 189-196.

40. Burgess, M.; Chenard, E.; Hernandez-Burgos, K.; Nagarjuna, G.; Assary, R. S.; Hui, J. S.; Moore, J. S.; Rodriguez-Lopez, J., Impact of Backbone Tether Length and Structure on the Electrochemical Performance of Viologen Redox Active Polymers. *Chem Mater* **2016,** *28* (20), 7362-7374.

41. Nagarjuna, G.; Hui, J.; Cheng, K. J.; Lichtenstein, T.; Shen, M.; Moore, J. S.; Rodriguez-Lopez, J., Impact of redox-active polymer molecular weight on the electrochemical properties and transport across porous separators in nonaqueous solvents. *J Am Chem Soc* **2014,** *136* (46), 16309-16.

42. Odom, S., Preventing Crossover in Redox Flow Batteries through Active Material Oligomerization. *ACS Cent Sci* **2018,** *4* (2), 140-141.

43. Doris, S. E.; Ward, A. L.; Baskin, A.; Frischmann, P. D.; Gavvalapalli, N.; Chenard, E.; Sevov, C. S.; Prendergast, D.; Moore, J. S.; Helms, B. A., Macromolecular Design Strategies for Preventing Active-Material Crossover in Non-Aqueous All-Organic Redox-Flow Batteries. *Angew Chem Int Ed* **2017,** *56* (6), 1595-1599.

44. Chai, J.; Lashgari, A.; Wang, X.; Williams, C. K., All-PEGylated redox-active metal-free organic molecules in non-aqueous redox flow battery. *J Mater Chem A* **2020**.

45. Ashraf Gandomi, Y.; Aaron, D. S.; Mench, M. M., Influence of Membrane Equivalent Weight and Reinforcement on Ionic Species Crossover in All-Vanadium Redox Flow Batteries. *Membranes* **2017,** *7* (2), 29.

46. Gandomi, Y. A.; Aaron, D.; Mench, M., Coupled membrane transport parameters for ionic species in all-vanadium redox flow batteries. *Electrochim Acta* **2016,** *218*, 174-190.

47. Trogadas, P.; Pinot, E.; Fuller, T. F., Composite, Solvent-Casted Nafion Membranes for Vanadium Redox Flow Batteries. *Electrochem Solid-State Lett* **2012,** *15* (1), A5.

48. Bauer, S.; Namyslo, J. C.; Kaufmann, D. E.; Turek, T., Evaluation of Options and Limits of Aqueous All-Quinone-Based Organic Redox Flow Batteries. *J Electrochem Soc* **2020,** *167* (11), 110522.

49. Murali, A.; Nirmalchandar, A.; Krishnamoorthy, S.; Hoober-Burkhardt, L.; Yang, B.; Soloveichik, G.; Prakash, G. K. S.; Narayanan, S. R., Understanding and Mitigating Capacity Fade in Aqueous Organic Redox Flow Batteries. *J Electrochem Soc* **2018,** *165* (7), A1193-A1203.

50. Kowalski, J. A.; Neyhouse, B. J.; Brushett, F. R., The impact of bulk electrolysis cycling conditions on the perceived stability of redox active materials. *Electrochem Commun* **2020,** *111*, 106625.

51. Kwabi, D. G.; Ji, Y.; Aziz, M. J., Electrolyte Lifetime in Aqueous Organic Redox Flow Batteries: A Critical Review. *Chem Rev* **2020,** *120* (14), 6467-6489.

52. Brushett, F. R.; Aziz, M. J.; Rodby, K. E., On lifetime and cost of redox-active organics for aqueous flow batteries. *Acs Energy Lett* **2020,** *5* (3), 879-884.

53. Yao, Y.; Lei, J.; Shi, Y.; Ai, F.; Lu, Y.-C., Assessment methods and performance metrics for redox flow batteries. *Nature Energy* **2021,** *6* (6), 582-588.

54. Wang, Y.; Kaur, A. P.; Attanayake, N. H.; Yu, Z.; Suduwella, T. M.; Cheng, L.; Odom, S. A.; Ewoldt, R. H., Viscous flow properties and hydrodynamic diameter of phenothiazine-based redox-active molecules in different supporting salt environments. *Phys Fluids* **2020,** *32* (8).

55. Burgess, M.; Hernandez-Burgos, K.; Schuh, J. K.; Davila, J.; Montoto, E. C.; Ewoldt, R. H.; Rodriguez-Lopez, J., Modulation of the Electrochemical Reactivity of Solubilized Redox Active Polymers via Polyelectrolyte Dynamics. *J Am Chem Soc* **2018,** *140* (6), 2093-2104.

56. Attanayake, N. H.; Liang, Z.; Wang, Y.; Kaur, A. P.; Parkin, S. R.; Mobley, J. K.; Ewoldt, R. H.; Landon, J.; Odom, S. A., Dual function organic active materials for nonaqueous redox flow batteries. *Mater Adv* **2021,** *2* (4), 1390-1401.

57. Zhang, J. L.; Corman, R. E.; Schuh, J. K.; Ewoldt, R. H.; Shkrob, I. A.; Zhang, L., Solution Properties and Practical Limits of Concentrated Electrolytes for Nonaqueous Redox Flow Batteries. *J Phys Chem C* **2018,** *122* (15), 8159-8172.

58. Macosko, C. W., Rheology Principles. *Measurements and Applications* **1994**.

59. Furst, E. M.; Squires, T. M., *Microrheology*. Oxford University Press: 2017.

60. Zhang, Y.; Xue, L.; Khabaz, F.; Doerfler, R.; Quitevis, E. L.; Khare, R.; Maginn, E. J., Molecular Topology and Local Dynamics Govern the Viscosity of Imidazolium-Based Ionic Liquids. *J Phys Chem B* **2015,** *119* (47), 14934-44.

61. Ewoldt, R. H.; Johnston, M. T.; Caretta, L. M., Experimental Challenges of Shear Rheology: How to Avoid Bad Data. In *Complex Fluids in Biological Systems*, Springer: 2015; pp 207-241.

62. Milshtein, J. D.; Kaur, A. P.; Casselman, M. D.; Kowalski, J. A.; Modekrutti, S.; Zhang, P. L.; Attanayake, N. H.; Elliott, C. F.; Parkin, S. R.; Risko, C.; Brushett, F. R.; Odom, S. A., High current density, long duration cycling of soluble organic active species for non-aqueous redox flow batteries. *Energ Environ Sci* **2016,** *9* (11), 3531-3543.

63. Attanayake, N. H.; Kowalski, J. A.; Greco, K. V.; Casselman, M. D.; Milshtein, J. D.; Chapman, S. J.; Parkin, S. R.; Brushett, F. R.; Odom, S. A., Tailoring Two-Electron-Donating Phenothiazines To Enable High Concentration Redox Electrolytes for Use in Nonaqueous Redox Flow Batteries. *Chem Mater* **2019,** *31* (12), 4353-4363.

64. Zhang, J. J.; Huang, J. H.; Robertson, L. A.; Shkrob, I. A.; Zhang, L., Comparing calendar and cycle life stability of redox active organic molecules for nonaqueous redox flow batteries. *J Power Sources* **2018,** *397*, 214-222.

65. Yuan, J. S.; Zhang, C. J.; Zhen, Y. H.; Zhao, Y. C.; Li, Y. D., Enhancing the performance of an all-organic non-aqueous redox flow battery. *J Power Sources* **2019,** *443*, 227283.

66. Narayana, K. A.; Casselman, M. D.; Elliott, C. F.; Ergun, S.; Parkin, S. R.; Risko, C.; Odom, S. A., N-Substituted Phenothiazine Derivatives: How the Stability of the Neutral and Radical Cation Forms Affects Overcharge Performance in Lithium-Ion Batteries. *Chemphyschem* **2015,** *16* (6), 1179-1189.

67. Luo, J.; Sam, A.; Hu, B.; DeBruler, C.; Wei, X.; Wang, W.; Liu, T. L., Unraveling pH dependent cycling stability of ferricyanide/ferrocyanide in redox flow batteries. *Nano Energy* **2017,** *42*, 215-221.

68. Goulet, M.-A.; Aziz, M. J., Flow Battery Molecular Reactant Stability Determined by Symmetric Cell Cycling Methods. *J Electrochem Soc* **2018,** *165* (7), A1466-A1477.

69. Potash, R. A.; McKone, J. R.; Conte, S.; Abruna, H. D., On the Benefits of a Symmetric Redox Flow Battery. *J Electrochem Soc* **2016,** *163* (3), A338-A344.

70. Duan, W. T.; Huang, J. H.; Kowalski, J. A.; Shkrob, I. A.; Vijayakumar, M.; Walter, E.; Pan, B. F.; Yang, Z.; Milshtein, J. D.; Li, B.; Liao, C.; Zhang, Z. C.; Wang, W.; Liu, J.; Moore, J. S.; Brushett, F. R.; Zhang, L.; Wei, X. L., "Wine-Dark Sea" in an Organic Flow Battery: Storing Negative Charge in 2,1,3-Benzothiadiazole Radicals Leads to Improved Cyclability. *ACS Energy Lett* **2017,** *2* (5), 1156-1161.

71. Yu, X.; Yu, W. A.; Manthiram, A., A Unique Single-Ion Mediation Approach for Crossover-Free Nonaqueous Redox Flow Batteries with a Na+ -Ion Solid Electrolyte. *Small Methods* **2019,** *4* (1), 1900697.

72. Yu, X.; Yu, W. A.; Manthiram, A., A mediator-ion nitrobenzene - iodine nonaqueous redox flow battery with asymmetric solvents. *Energy Storage Mater* **2020,** *29*, 266-272.

73. Shrestha, A.; Hendriks, K. H.; Sigman, M. S.; Minteer, S. D.; Sanford, M. S., Realization of an Asymmetric Non-Aqueous Redox Flow Battery through Molecular Design to Minimize Active Species Crossover and Decomposition. *Chem Eur J* **2020,** *26* (24), 5369-5373.

74. Vaid, T. P.; Sanford, M. S., An organic super-electron-donor as a high energy density negative electrolyte for nonaqueous flow batteries. *Chem Commun* **2019,** *55* (74), 11037-11040.

75. Howe, P. W. A., Suppression of Protonated Organic Solvents in NMR Spectroscopy Using a Perfect Echo Low-Pass Filtration Pulse Sequence. *Anal Chem* **2018,** *90* (7), 4316-4319.

76. Robertson, L. A.; Shkrob, I. A.; Agarwal, G.; Zhao, Y.; Yu, Z.; Assary, R. S.; Cheng, L.; Moore, J. S.; Zhang, L., Fluorescence-enabled self-reporting for redox flow batteries. *ACS Energ Lett* **2020**.

77. Zhao, E. W.; Liu, T.; Jonsson, E.; Lee, J.; Temprano, I.; Jethwa, R. B.; Wang, A.; Smith, H.; Carretero-Gonzalez, J.; Song, Q.; Grey, C. P., In situ NMR metrology reveals reaction mechanisms in redox flow batteries. *Nature* **2020,** *579* (7798), 224-228.

78. Zhao, E. W.; Jonsson, E.; Jethwa, R. B.; Hey, D.; Lyu, D.; Brookfield, A.; Klusener, P. A. A.; Collison, D.; Grey, C. P., Coupled In Situ NMR and EPR Studies Reveal the Electron Transfer Rate and Electrolyte Decomposition in Redox Flow Batteries. *J Am Chem Soc* **2021,** *143* (4), 1885-1895.